Photorefractivity in Polymer-Stabilized Nematic Liquid Crystals

Gary P. Wiederrecht[†] and Michael R. Wasielewski*[,†,‡]

Contribution from the Chemistry Division, Argonne National Laboratory, Argonne, Illinois 60439-4831, and Department of Chemistry, Northwestern University, Evanston, Illinois 60208-3113

Received November 26, 1997

Abstract: The charge generation and transport properties of nematic liquid crystals doped with electron donors and acceptors are shown to be strongly modified by the addition of low concentrations of a polymeric electron acceptor. These new liquid crystalline composites exhibit significantly enhanced photorefractive properties. The new composites are produced by polymerizing a small quantity of a 1,4:5,8-naphthalenediimide electron acceptor functionalized with an acrylate group in an aligned nematic liquid crystal. Photopolymerization creates an anisotropic gellike medium in which the liquid crystal is free to reorient in the presence of a space-charge field while maintaining charge-trapping sites in the polymerized regions of the material. The presence of these trapping sites results in the observation of longer lived, higher resolution holographic gratings in the polymer-stabilized liquid crystals than observed in nematic liquid crystals alone. These gratings display Bragg regime diffraction. Asymmetric beam coupling, photoconductivity, and four-wave mixing experiments are performed to characterize the photophysics of these novel materials. The mechanism of charge transport in the polymer-stabilized liquid crystals is also discussed.

Introduction

The development of new photorefractive materials has accelerated over the past several years. The photorefractive effect is a light-induced change in the refractive index of a nonlinear optical material. It results from the creation of an electric field produced by directional charge transport over macroscopic distances. If the material is electrooptic, the electric (or space-charge) field can modulate the refractive index of the sample. When the photorefractive effect is properly optimized, the material can be used for a variety of optical signal processing techniques.[1−3] As a consequence of their outstanding optical quality, photorefractive performance, and commercial availability, inorganic ferroelectric materials, such as barium titanate and lithium niobate, have been used to produce photorefractive holographic data storage systems.[4] Nevertheless, the development of new organic materials that respond over a wider range of wavelengths and that have significantly lower cost than inorganic single crystals would dramatically enhance the versatility of the photorefractive effect. In this pursuit, photorefractive polymers and liquid crystals (LCs) have recently been explored.[5−15] Photorefractive polymers and LCs are generally composite materials that possess additives that serve to induce the photorefractive effect. The additives for the polymers are typically a nonlinear optical (NLO) chromophore, an electron donor or acceptor to photogenerate mobile charges within the composite, and a plasticizer for lowering the glass transition temperature to permit reorientation of the NLO chromophore. Another strategy incorporates all of the required species for photorefractivity onto a polymer backbone.[9,16−18] The additives in LCs are electron donors and acceptors that can be easily oxidized and reduced, respectively, to photogenerate mobile charges in the LC. No NLO dopants are necessary to induce electrooptic character within the LCs because the electrooptic mechanism in these materials is not derived from the electrooptic effect observed in noncentrosymmetric systems, but through the orientational enhancement effect.[5] This effect relies on the ability of birefringent molecules to reorient in the presence of a space charge field. Interestingly, the orientational enhancement effect in many of the most recent polymeric systems has been shown to be responsible for the majority of the photorefractive gain, a result of the low glass transition temperatures of the polymers. The reorientation of the director within nematic LCs is not as straightforward a process as the reorientation of the NLO chromophore within the polymeric systems because the space-charge fields induce a variety of torques and flows within the nematic material.[19] Nonetheless,

[†] Argonne National Laboratory.
[‡] Northwestern University.

(1) Feinberg, J. *Physics Today* **1988**, Oct, 46−52.
(2) Giuliano, C. R. *Physics Today* **1981**, April, 27−35.
(3) Gunter, P.; Huignard, J. P. *Photorefractive Materials and Their Applications 1: Fundamental Phenomena*; Springer-Verlag: Berlin, 1988.
(4) Psaltis, D.; Mok, F. *Sci. Am.* **1995**, Nov, 70.
(5) Moerner, W. E.; Silence, S. M. *Chem. Rev.* **1994**, *94*, 127−155.
(6) Zhang, Y.; Cui, Y.; Prasad, P. N. *Phys. Rev. B* **1992**, *46*, 9900.
(7) Volodin, B. L.; Kippelen, B.; Meerholz, K.; Javidi, B.; Peyghambarian, N. *Nature* **1996**, *383*, 58−60.
(8) Ducharme, S.; Scott, J. C.; Twieg, R. J.; Moerner, W. E. *Phys. Rev. Lett.* **1991**, *66*, 1846−1849.
(9) Yu, L.; Chan, W. K.; Peng, A.; Gharavi, A. *Acc. Chem. Res.* **1996**, *29*, 13-21.
(10) Khoo, I. C.; Li, H.; Liang, Y. *Opt. Lett.* **1994**, *19*, 1723−25.
(11) Rudenko, E. V.; Sukhov, A. V. *JETP Lett.* **1994**, *59*, 142−46.
(12) Wiederrecht, G. P.; Yoon, B. A.; Wasielewski, M. R. *Science* **1995**, *270*, 1794−97.
(13) Wiederrecht, G. P.; Yoon, B. A.; Wasielewski, M. R. *Adv. Mater.* **1996**, *8*, 535−39.
(14) Wiederrecht, G. P.; Yoon, B. A.; Wasielewski, M. R. *Synth. Met.* **1997**, *84*, 901−2.
(15) Wiederrecht, G. P.; Yoon, B. A.; Svec, W. A.; Wasielewski, M. R. *J. Am. Chem. Soc.* **1997**, *119*, 3358.
(16) Kippelen, B.; Tamura, K.; Peyghambarian, N.; Padias, A. B.; Jr., H. K. H. *Phys. Rev. B* **1993**, *48*, 10710−18.
(17) Zhao, C.; Park, C.-K.; Prasad, P. N.; Zhang, Y.; Ghosal, S.; Burzynski, R. *Chem. Mater.* **1995**, *7*, 1237−42.
(18) Li, L.; Chittibabu, K. G.; Chen, Z.; Chen, J. I.; Marturunkakul, S.; Kumar, J.; Tripathy, S. K. *Opt. Comm.* **1996**, *125*, 257−61.
(19) Khoo, I. C. *IEEE J. Quantum Elec.* **1996**, *32*, 525−534.

S0002-7863(97)04033-X CCC: $15.00
Published on Web 03/20/1998

the end result is the same: a large refractive index change is created due to the high birefringence of the reorienting media within the space-charge field.

It would be desirable to combine the very large reorientational effects found in LCs with the charge-transport characteristics of polymers to produce longer lived index gratings. Liquid crystal polymer dispersions are already of great interest for their electrooptic applications. The dispersions are usually studied with a high concentration of polymer and a smaller concentration of LC molecules that separate into droplets. Such materials are opaque due to the random orientations of the LC directors of the droplets until an electric field is applied. The resulting alignment of the LC directors within each droplet along the electric field produces a transparent material. Such materials are clearly of interest for optical shutters, and orientational photorefractivity has recently been reported in them.[20,21] However, an entirely different type of material results if a small amount (1−2 wt %) of a polymeric monomer is dissolved in an aligned LC and subsequently photopolymerized with UV radiation in the presence of a photoinitiator. The resulting material is comparable to an anisotropic gel.[22−24] Such materials are referred to as polymer-stabilized liquid crystals (PSLCs) and have been discussed most often in reference to the development of shock-resistant LC displays. The birefringence of the nematic LCs is by and large preserved following polymerization because the monomers are rodlike acrylates that align well with the LC director.

We report here the preparation and characterization of a polymer-stabilized liquid crystal as a new type of organic photorefractive material. It is designed to maintain the high birefringence and reorientation characteristics typical of LCs but permits much smaller photorefractive grating fringe spacings by altering the charge transport properties of LCs to include charge trapping effects. The smaller fringe spacings produce a photorefractive grating in a nematic LC that operates in the thick grating (Bragg diffraction) regime. The smaller fringe spacings are achieved through the incorporation of easily reduced electron acceptors into the polymer that alter the charge transport and charge-trapping characteristics of the diffusing ions that create the space-charge field.

Results

Preparation of Polymer-Stabilized Liquid Crystal Composites. The PSLCs must be photoconductive in order to generate the space-charge field necessary for photorefractivity. Therefore, easily oxidized and reduced dopants must be added to produce efficient photoinduced charge generation and charge migration over macroscopic distances. With this in mind, the building blocks that make up the PSLCs are shown in Figure 1. The nematic LC is a eutectic mixture of 35% (weight %) 4′-(*n*-octyloxy)-4-cyanobiphenyl (8OCB) and 65% 4′-(*n*-pentyl)-4-cyanobiphenyl (5CB). The LC is doped with perylene (PER), which acts as the electron donor and the light absorbing chromophore (2×10^{-3}M). Perylene has a broad absorption band that peaks at 443 nm and permits the use of the 514 nm line of an Ar^+ laser beam to produce the photorefractive effect. Perylene is also easily oxidized at 0.8 V vs SCE. The sample

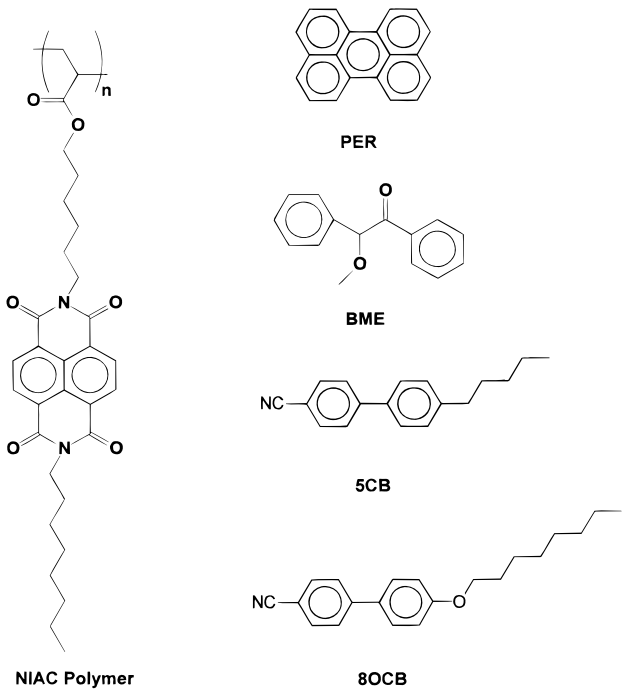

Figure 1. Components of the photorefractive polymer-stabilized liquid crystal.

is also doped with 2% (mol %) of NIAC, which is an acrylate monomer containing the easily reduced 1,4:5,8-naphthalenediimide moiety (−0.5 eV vs SCE). Given the 2.8 eV lowest excited singlet-state energy of PER, the free energy for photogeneration of solvent separated ions via the singlet state is −1.5 eV.[13] Finally, 0.5% (mol %) of benzoin methyl ether (BME) is added to photoinitiate polymerization of the NIAC.

The synthesis of NIAC is shown in Scheme 1. The preparation of *N*-(*n*-octyl)naphthalene-1,8-imide-4,5-dicarboxylic anhydride (**2**) was presented previously.[25] Compound **2** is refluxed in dry DMF with 6-amino-1-hexanol to give *N*-(*n*-octyl)-*N*′-(6-hydroxyhexyl)naphthalene-1,8:4,5-diimide (**3**) in 67% yield. Esterification of the terminal alcohol with acryloyl chloride gives NIAC in 64% yield.

Photorefractivity in Polymer-Stabilized Liquid Crystals. The geometry of the beam-coupling experiment is illustrated in Figure 2. Two coherent, 2.5 mW, 514-nm beams from a continuous wave Ar^+ laser were overlapped in the sample. The beams were unfocused and had a 1/*e* diameter at the sample of 2.5 mm. Voltages of up to 2 V were applied to the polymerized samples, producing applied electric fields up to 800 V/cm. Asymmetric beam coupling was only observed in the presence of a dc-applied electric field, eliminating the possibility of beam coupling due to thermal or absorption gratings. Application of a 2V, 100 Hz ac field also did not result in any observed beam coupling. In addition, the diffracted spots only appeared with extraordinary (p) polarized beams, ensuring that the grating was due to reorientation of the LC molecules in the plane defined by the two writing beams, consistent with reorientation due to the space-charge field. Photorefractivity is observed only in the birefringent nematic phase of the LC, not in its isotropic phase. For those experiments performed in the multiple diffraction regime (i.e., $\Lambda > \sim 8\,\mu$m), beam coupling manifested itself as an increase in the intensity of all of the diffracted and undiffracted light from one beam and a corresponding drop in the intensity of the other beam and its diffracted beams.

(20) Golemme, A.; Volodin, B. L.; Kippelen, B.; Peyghambarian, N. *Opt. Lett.* **1997**, *22*, 1226−28.
(21) Ono *Opt. Lett.* **1997**, *22*, 1144−46.
(22) Guymon, C. A.; Hoggan, E. N.; Walba, D. M.; Clark, N. A.; Bowman, C. N. *Liq. Cryst.* **1995**, *19*, 719−27.
(23) Hikmet, R. A. M. *J. Appl. Phys.* **1990**, *68*, 4406−4412.
(24) Rajaram, C. V.; Hudson, S. D.; Chien, L. C. *Chem. Mater.* **1995**, *7*, 2300−08.
(25) Wiederrecht, G. P.; Niemczyk, M. P.; Svec, W. A.; Wasielewski, M. R. *J. Am. Chem. Soc.* **1996**, *118*, 81−88.

Scheme 1

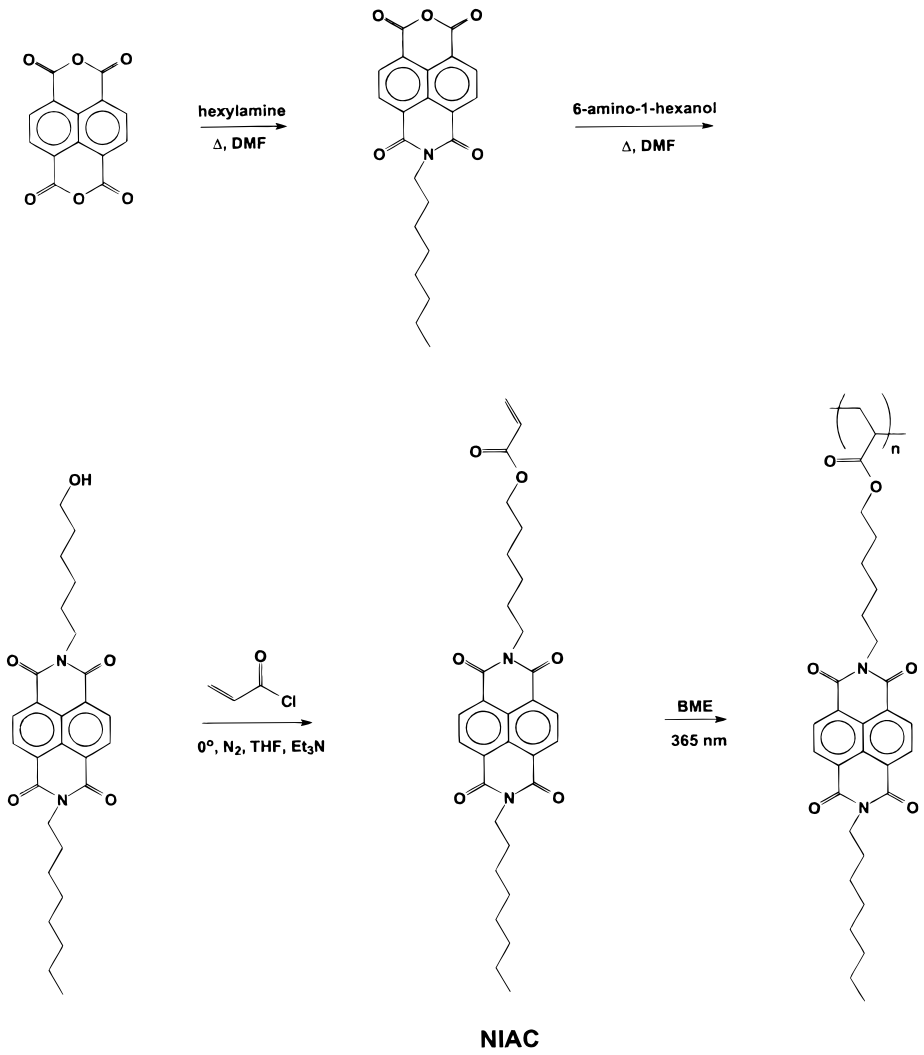

NIAC

The improved photorefractive grating resolution due to polymer stabilization is illustrated by the asymmetric beam-coupling measurements shown in Figure 3. The unpolymerized samples do not show any measurable beam coupling for fringe spacings (Λ) below 8 μm, whereas the polymerized samples exhibit beam coupling down to $\Lambda = 2.5$ μm. We found that the samples polymerized for 2 min exhibited the highest beam coupling ratios at small fringe spacings. Samples that were polymerized for longer times exhibited reduced beam coupling at all fringe spacings, whereas those polymerized for only 1 min showed high beam coupling at larger fringe spacings, but no beam coupling at shorter fringe spacings in a manner similar to the unpolymerized samples. The dependence of two-beam coupling on polymerization time suggests that optimal photorefractivity is observed when polymerization of NIAC is not quantitative and that unpolymerized monomers are present along with longer chains of polymerized NIAC. The incomplete polymerization permits mobile PER cations and monomeric NIAC anions that provide for bulk charge transport to coexist with the less mobile polymerized NIAC electron-acceptor trapping sites. Figure 4 shows the kinetics of beam coupling at $\Lambda = 4.8$ μm for samples that were polymerized for 2 min. The inset to Figure 4 shows the beam coupling at the smallest fringe spacing of 2.5 μm.

The photorefractive rise (τ_{pr}) and decay (τ_{pd}) times vs Λ, as measured by the four wave-mixing experiments, are shown in Figure 5a,b for the polymerized and unpolymerized samples, respectively. The decay times are measured following the blockage of either one of the writing beams. Note that the rise times of the photorefractive gratings in the polymerized samples are always faster than the decay times when one beam is blocked for all but the smallest three fringe spacings. Conversely, for the unpolymerized samples, the decay times are always faster than the rise times even for the large fringe spacings studied. Therefore, the polymerized samples clearly produce a more stable photorefractive grating, and as a result, smaller fringe spacings can be attained.

The time-resolved photoconductivity measurements shown in Figure 6 give further support for a difference in photoinduced charge transport in the polymerized samples vs the unpolymerized samples. For an incident laser power of 100 mW/cm^2 and a spot size of 2.5 mm, the decay time of the photoconductivity for the unpolymerized samples is 7.4 s, whereas the photoconductivity of the polymerized samples does not significantly drop over a 30 s period. Also, the photoconductivity of the polymerized sample is nearly twice that of the unpolymerized samples even at the peak of the unpolymerized photoconductive response. The unnormalized values for the dark conductivity in both samples is 1.7×10^{-10} S cm^{-1}. The photoconductivity is 5.8×10^{-11} S cm^{-1} for the unpolymerized sample and 1.1×10^{-10} S cm^{-1} for the PSLC at an optical intensity of 2 W cm^{-2}.

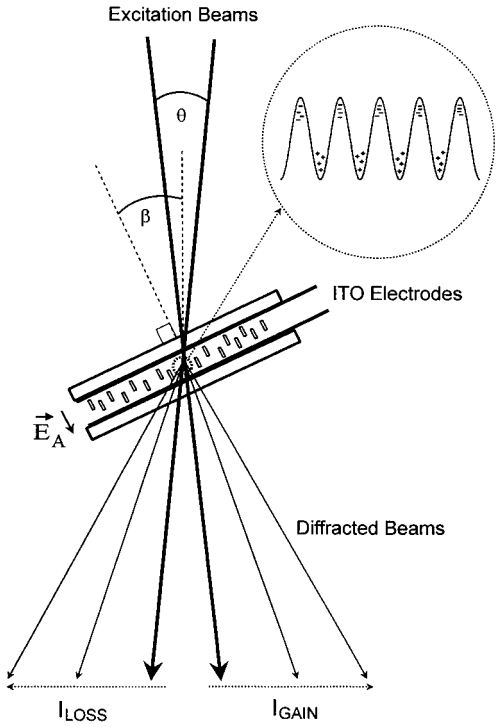

Figure 2. Schematic of the experimental geometry. The sample is tilted at an angle $\beta = 30°$ relative to the bisector of the two beams. This permits charge migration along the grating wavevector, which results in a sinusoidal space charge field. A phase grating results from the influence of the space-charge field on the orientational configuration of the birefringent LC molecules. The beams are p-polarized in the plane of the page. E_A is the applied electric field.

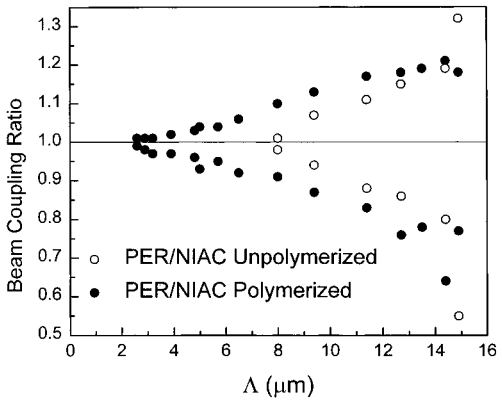

Figure 3. Beam coupling for the PSLC composite and unpolymerized LC. Beam coupling in the PSLC is observed down to 2.5 μm for an applied voltage of 1.8 V.

Discussion

To determine whether the grating is a thin (Raman-Nath) or volume (Bragg) grating, the following well-known parameter can be used[26]

$$Q = \frac{2\pi D\lambda}{\Lambda^2 n} \tag{1}$$

where λ is the wavelength of the light, n is the index of refraction, and D is the thickness of the grating ($D = d/\cos\beta$, where d is the cell thickness). For $Q \ll 1$, the grating is considered to be a plane grating, and for $Q \gg 1$, a volume grating is created. Although the literature does not appear to specifically designate an exact value for Q in which the thick grating regime is reached, the most rigorous treatments suggest that Q values of 10 are required to produce a true volume hologram.[27] For our samples, $Q = 10$ is achieved for $\Lambda = 2.6$ μm, when $D = 26$ μm/cos 30° = 30 μm, and $n = 1.5$. At this fringe spacing, our samples still exhibit a small amount of beam coupling (about ±1%), so the PSLCs can be considered to be

(26) Eichler, H. J.; Gunter, P.; Pohl, D. W. *Laser-Induced Dynamic Gratings*; Springer-Verlag: Berlin, 1986.

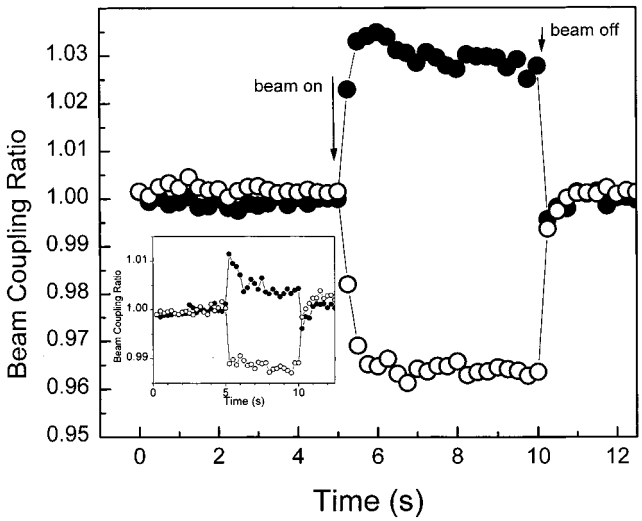

Figure 4. Kinetics of asymmetric beam coupling within the PSLC for $\Lambda = 4.8$ μm. The inset shows the beam coupling kinetics for $\Lambda = 2.5$ μm: beam 1, ●; beam 2, ○.

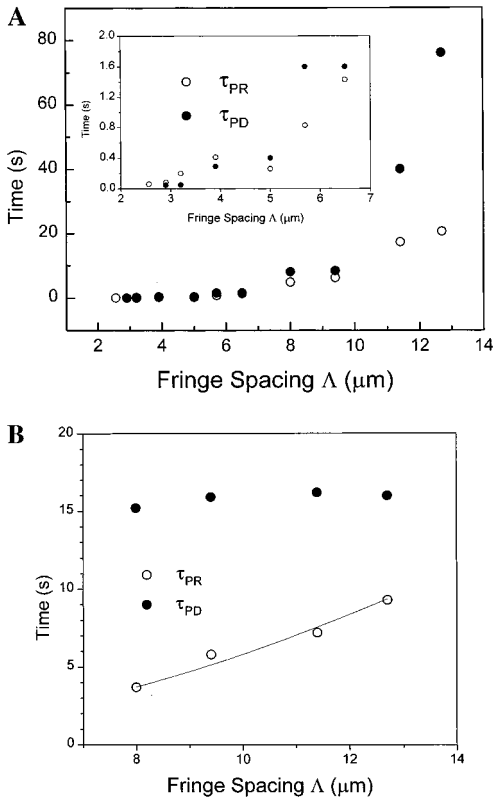

Figure 5. Rise, τ_{PR}, and decay times τ_{PD} of the photorefractive grating vs Λ for the (a) PSLC and the (b) unpolymerized LC. The inset in (a) is a magnification of the smallest fringe spacings studied. The unpolymerized LC decay times exhibit a quadratic dependence on fringe spacing, consistent with an ion diffusion, whereas the PSLCs show a steeper dependence vs Λ.

(27) Ja, Y. H. *Elect. Lett.* **1981**, *17*, 488−9.

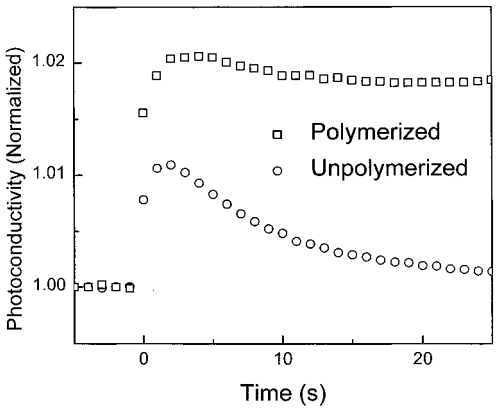

Figure 6. Improved photoconductivity of the PSLC relative to the LC.

operative in the thick grating regime. This compares favorably to the best case scenario exhibited by the LCs with no polymer stabilization, where beam coupling is observed for fringe spacings no smaller than $\Lambda = 8\ \mu$m, giving $Q = 1$.

Given that the samples operate in the nominally thick grating regime, the net photorefractive gain (Γ) can be calculated assuming an exponential dependence on the thickness of the sample[5]

$$\Gamma = \frac{1}{D}\left[\ln\frac{I_{12}}{I_1} - \ln\left(2 - \frac{I_{12}}{I_1}\right)\right] - \alpha \qquad (2)$$

where α is the sample absorbance, I_1 is the intensity of beam 1 in the absence of beam 2, and I_{12} is the intensity of beam 1 with beam 2 applied. The absorbance of the sample at 514 nm is 0.003, resulting in values for α of only 1 cm^{-1}. Therefore, for $\Lambda = 2.5\ \mu$m a net photorefractive gain of $\Gamma = 5$ cm^{-1} results. For somewhat less rigorous treatments of the Q value, higher photorefractive gains are calculated. For example, some researchers suggest that the condition $\Lambda^2 \approx D\lambda$ is sufficient for the thick grating regime to be reached, so that for $\Lambda = 4\ \mu$m ($Q = 4$) beam coupling of $\pm 3\%$ is observed and the net photorefractive gain is 15 cm^{-1}.[21] It should be noted that impressive photorefractive gains as high as 2890 cm^{-1} are currently being reported in LCs, but these materials do not operate in the thick grating regime[28] and eq 2 may not be strictly applicable.[29] We have highlighted this potential problem previously in reporting both beam-coupling ratios and calculated photorefractive gains in our own work.[12]

The beam coupling, four-wave mixing, and photoconductivity data indicate that the mechanism for charge transport within the PSLCs differs from that within the unpolymerized samples. For the unpolymerized samples, the primary mechanism for creating a space-charge field is the difference in diffusion constants of the cations and anions:[19]

$$E_{sc} = \frac{k_B T \Lambda}{4\pi e_o}\frac{D^+ - D^-}{D^+ + D^-}\frac{\sigma_{ph}}{\sigma_{ph} + \sigma_d}\sin\frac{\Lambda x}{2\pi} \qquad (3)$$

where D^+ and D^- are the diffusion coefficients of the cations and anions, respectively, k_B is the Boltzmann constant, T is the temperature, σ_{ph} is the photoconductivity, σ_d is the dark conductivity, and e_o is the electronic charge. Equation 3 assumes that $I_1 = I_2$. Further support for ion diffusion as the mechanism for photorefractivity in the unpolymerized samples is the quadratic dependence of the grating decay time vs fringe spacing, as shown in Figure 5b.[19,26] However, the data for the polymerized samples clearly indicate a decay time dependence vs Λ that is far greater than quadratic.

The photorefractive data from the polymerized samples can be explained in terms of a model in which the polymerized NIAC electron acceptor functions as an electron-trap site. The existence of less mobile electron traps can explain the smaller fringe spacings at which asymmetric two-beam coupling is observed. Since Debye diffusion lengths are proportional to $D^{1/2}$, the drop in the best value of Λ from 8 μm for the unpolymerized samples to 2.5 μm for the PSLCs indicates that the polymerized NIAC functions as an electron trap with an average diffusion constant that is approximately 1 order of magnitude smaller than that of monomeric NIAC$^-$. In this model, it is critical that the polymerization is not quantitative so that mobile monomers of NIAC$^-$ are present to carry out charge transport between the fringes of the optical interference pattern.

At the same time, the polymerized NIAC may play a role in improving the photoconductivity of the PSLCs, as reported above and illustrated in Figure 6. Improvements in the photoconductivity are due to either an increase in the quantum efficiency of mobile charge generation (ϕ) or an increase in the mobility of the ions (μ) because $\sigma_{ph} \propto \phi\mu$.[30] If we assume that the acrylate chain on the monomeric NIAC acceptor does not significantly alter the mobility of the reduced NIAC monomer relative to the corresponding *N*,*N*-di-*n*-octyl derivative previously examined,[12] the quantum efficiency of charge generation must improve. Collisions of PER* with NIAC create PER$^+$−NIAC$^-$ ion pairs, and a fraction of the population of these initial ion pairs form the solvent-separated ions necessary for bulk charge transport. If the initial PER$^+$−NIAC$^-$ ion pair is formed on a polymerized NIAC strand, there is a greatly increased probability that charge hopping will occur to other NIAC molecules on the same polymer strand. Thus, an additional mechanism for creating solvent-separated ions is present in the PSLCs that is not present in conventional LCs.

Another significant difference between the PSLCs and LCs is the behavior of the decay of the photorefractive gratings with both beams blocked compared to one beam blocked. The photorefractive grating decays very quickly for the PSLCs when both writing beams are blocked, whereas slower grating decay is observed when only one beam is blocked, as measured by four-wave mixing experiments shown in Figure 7. In fact, the lifetimes of the gratings are enhanced by more than 1 order of magnitude when one beam is incident on the sample. No such lifetime increase is observed for photorefractive gratings in unpolymerized LCs, illustrated by the inset to Figure 7. These experiments show that a photoinduced process occurs in the PSLCs that promotes charge separation and inhibits charge recombination.

One possible explanation for these observations is suggested by focusing on the electron-transfer equilibrium that occurs between monomeric NIAC$^-$ and the polymerized NIAC traps. After the grating is formed, removal of both laser beams from the sample results in rapid charge recombination between monomeric NIAC$^-$ and PER$^+$ because of the greater mobility of monomeric NIAC$^-$ relative to that of polymerized NIAC$^-$. The rapid depletion of monomeric NIAC$^-$ in the PSLCs results in a shift in the charge equilibrium between monomeric NIAC

(28) Khoo, I. C.; Guenther, B. D.; Wood, M. V.; Chen, P.; Shih, M.-Y. *Opt. Lett.* **1997**, *22*, 1229−31.

(29) Moerner, W. E.; Grunnet-Jepsen, A.; Thompson, C. L. *Annu. Rev. Mater. Sci.* **1997**, *27*, 585−623.

(30) Scott, J. C.; Pautmeier, L. T.; Moerner, W. E. *J. Opt. Soc. Am. B* **1992**, *9*, 2059−64.

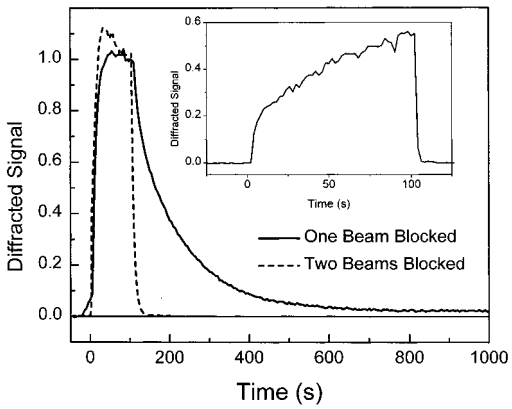

Figure 7. Difference in decay kinetics for one beam blocked vs two beams blocked in the PSLC. The lifetime of the grating is enhanced when one beam is incident on the sample. The inset shows the decay kinetics for the unpolymerized LC when one beam is incident on the sample. No enhancement of the grating lifetime is observed. Both beams are incident on the sample at $t = 0$ and either one or both beams are blocked as specified above at $t = 100$ s. $\Lambda = 12.7$ μm.

and polymerized $NIAC^-$ to move charge onto the more mobile monomeric NIAC, which in turn transfers the electron back to PER^+. This process most likely occurs in parallel with direct electron transfer from polymerized $NIAC^-$ to PER^+. On the other hand, when a single laser beam remains incident on the grating, PER^+ and $NIAC^-$ are generated throughout the existing grating. This laser beam generates excess $NIAC^-$, which shifts the equilibrium for electron transfer between monomeric NIAC and polymerized $NIAC^-$ to favor retention of charge on polymerized NIAC. Thus, the previously generated spatial grating due to electron trapping on polymerized NIAC is preserved for a longer period of time.

Conclusions

We have shown that PSLCs are capable of forming photorefractive gratings that operate in the thick grating (Bragg) regime. Polymer stabilization alters the charge-transport and trapping characteristics of LCs, resulting in longer lived gratings, while maintaining the advantages of high orientational birefringence within LCs. Furthermore, very low applied electric fields (800 V/cm) and low optical intensities (100 mW/cm^2) are required to create large photorefractive effects in these materials. It is expected that further optimization of the photophysical and redox potentials of the donor−acceptor additives and of their incorporation into the polymer structure within the PSLCs will continue to improve the photorefractive performance of these materials.

Experimental Section

Synthesis of NIAC. Proton NMR spectra were obtained on a Bruker DMX-500 500 MHz spectrometer. Mass spectra were obtained with a Kratos MALDI spectrometer. UV−vis spectra were obtained with a Shimadzu UV-1601 spectrometer. Merck silica gel 60 was used for column chromatography.

***N*-(*n*-Octyl)-*N*′-(6-hydroxyhexyl)naphthalene-1,8:4,5-diimide, 3.** *N*-(*n*-octyl)naphthalene-1,8-imide-4,5-dicarboxylic anhydride, **2**[25] (500 mg, 1.3 mmol), and 6-amino-1-hexanol (340 mg, 2.9 mmol) were refluxed in dry DMF (25 mL) for 2 h. Upon cooling, **3** precipitated out of the solution and was suction filtered. **3** was washed with 10 mL of CH_3OH and subsequently with petroleum ether (10 mL × 2). Further purification was not necessary, and **3** was isolated in 67% yield (429 mg, 0.890 mmol): ^{1}H NMR ($CDCl_3$) δ 8.76 (s, 4H, Ar), 4.21 (t, 2H, $J = 7.7$ Hz, hexyl-1), 4.19 (t, 2H, $J = 8.0$ Hz, octyl-1), 3.65 (t, 2H, $J = 6.5$ Hz, hexyl-6), 1.76 (m, 4H, octyl and hexyl chains), 1.45 (m, 16H, octyl and hexyl chains), 0.88 (t, 3H, octyl-8); MS *m*/*e* calcd 479.6, found 480.0.

***N*-(*n*-Octyl)-*N*′-[6-(acryloyloxy)hexyl]naphthalene-1,8:4,5-diimide, NIAC.** Imide **3** (270 mg, 0.57 mmol) was added to dry THF(50 mL) containing 4% (vol) triethylamine. The solution was cooled to 0 °C under N_2 and stirred, while acryloyl chloride (62 mg, 0.69 mmol) was added dropwise. After 2 h, 100 mL of CH_2Cl_2 was added, and the organic layer was washed with water (100 mL × 3). The solvent was evaporated, and purification by silica gel chromatography (5% acetone in CH_2Cl_2) gave NIAC in 64% yield (194 mg, 360 μmol): ^{1}H NMR($CDCl_3$) δ 8.76 (s, 4H, Ar), 6.39 (d of d, 1H, $J = 17.4$, 1.5 Hz, vinyl), 6.11 (d of d, 1H, $J = 17.3$, 10.4 Hz, vinyl), 5.81 (d of d, 1H, $J = 10.4$, 1.5 Hz, vinyl), 4.21 (t, 2H, $J_{12} = 5.9$ Hz, hexyl-1), 4.19 (t, 2H, $J = 6.0$ Hz, octyl-1), 4.16 (t, 2H, $J = 6.7$ Hz, hexyl-6), 1.74 (m, 6H, octyl and hexyl chains), 1.38 (m, 14H, octyl and hexyl chains), 0.88 (t, 3H, $J = 6.8$ Hz octyl-8); MS *m*/*e* calcd 533.6, found 533.7.

Assembly of Cells and Photopolymerization. The sample cells were prepared as follows: Indium−tin oxide (ITO)-coated glass slides (Delta Technologies, 100 Ω/sq 90% transparent) were treated with the surfactant octadecyltrichlorosilane to induce LC director alignment perpendicular to the plane of the glass slides (homeotropic alignment).[31] Teflon spacers were used between the ITO glass slides to create 26 μm thick optical cells. The LC composite was drawn into the cell by capillary action, and alignment occurred in approximately 30 min. Photopolymerization of the acrylate monomers was performed within the aligned LC samples with 365 nm light at an intensity of 2 mW/cm^2. Polymerization times of 1, 2, 4, and 6 min were utilized. The polymerized samples appeared slightly more hazy at high angles of incidence than the unpolymerized samples. Pressure applied to the cell by hand squeezing did not misalign the material as is the case with the unpolymerized samples.

Four-wave mixing and photoconductivity measurements were also performed to characterize the samples. For the four wave mixing experiments, a third p-polarized HeNe laser beam was arranged in boxcar pattern and the diffracted HeNe laser beam that constituted the fourth "corner" of the box was monitored.[32] For the photoconductivity experiments, a Keithley model 485 picoammeter was used. Although the photocurrent is relatively low (~10^{-9} A) for incident CW powers of 100 mW/cm^2, the 10 MΩ resistance of the samples resulted in good reproducibility for the photocurrent measurements. Both experiments were digitized using a National Instruments AT-MIO-16 A/D board in conjunction with LabWindows/CVI software on a Gateway 486 33 MHz PC.

Acknowledgment. We gratefully acknowledge support from the Office of Computational and Technology Research, Division of Advanced Energy Projects and Technology Research, U.S. Department of Energy, under Contract No. W-31-109-ENG-38.

JA974033Z

(31) Khoo, I. C. *Liquid Crystals: Physical Properties and Nonlinear Optical Phenomena*; Wiley: New York, 1995.
(32) Nelson, K. A.; Casalegno, R.; Miller, R. J. D.; Fayer, M. D. *J. Chem. Phys.* **1982**, *77*, 1144−52.